Journal of Applied Mechanics and Technical Physics, Vol. 50, No. 3, pp. 361–370, 2009

ON STABILIZATION OF IMPLOSION OF CONDENSED LINERS

A. M. Buiko, S. F. Garanin, V. V. Zmushko,
V. M. Kalashnikov, V. N. Mokhov,
N. V. Sokolova, and V. B. Yakubov

UDC 537.84

This paper considers various experimental designs on the Atlas facility to study the physics of liners and determine the optimum conditions of their stable motion. In one of the versions, in comparison with the Liner Demonstration series of experiments, in which unstable liner motion was observed, it is proposed to reduce the initial liner radius without changing its mass, which, according to two-dimensional calculations, should to lead to more stable motion of the liner with unchanged velocity. It is also proposed to perform an experiment in which periodic perturbations at a certain wavelength are created on the outer surface of the liner with a simultaneous increase in its thickness. According to calculations, the growth of chaotic perturbations is stabilized in this case with the preservation of the liner velocity.

Key words: *implosion of condensed liners, Rayleigh–Taylor instability, two-dimensional magnetohydrodynamic calculations.*

INTRODUCTION

In recent decades, significant progress has been made in the theoretical and experimental physics of high energy density. Using condensed liners accelerated by powerful pulsed facilities in Z-pinch geometry is an important line of research [1–4]. Such liners are used in measurement of shock adiabat of condensed materials [2, 3]; in studies of the isentropic compression of materials; in studies of the dynamic strength characteristics of various materials based on measuring perturbation amplitudes in accelerated liners [4]; in modeling the operation of various devices and their fragments at high velocities and pressures; in studies of gravitational turbulent mixing of accelerated materials with various density at their interface.

Condensed liners accelerated by powerful pulsed facilities are also used for plasma compression for the purpose of its ignition or designing powerful radiation sources based on the MAGO/MTF concept [5, 6].

To use condensed liners in the studies listed above, it is necessary to attain high energy densities, which, in turn, requires the attainment of velocities of condensed liners of the order of 1 cm/μsec or higher. To attain such velocities, it is common to use magnetic fields of the megagauss range, which leads to melting or even vaporization of part of the liner (skin-layer) and its conversion to a plasma [7] and, hence, to a loss of its strength. This gives rise to conditions for the development of Rayleigh–Taylor and sausage instabilities in that part of the liner. The development of these instabilities can lead to the occurrence of an inhomogeneous state of the liner, which deteriorates the conditions of its use and, sometimes, leads to its failure.

The indestructibility conditions of accelerated liquid or gas liners under Rayleigh–Taylor instability conditions are estimated using a simple, though rough, criterion — the ratio of the distance traveled by the liner to its thickness. It is difficult to accelerate a liner so that it travels a distance exceeding ten its thicknesses. In the case of

All-Russia Scientific Research Institute of Experimental Physics, Sarov 607190; sfgar@vniief.ru. Translated from Prikladnaya Mekhanika i Tekhnicheskaya Fizika, Vol. 50, No. 3, pp. 3–14, May–June, 2009. Original article submitted November 8, 2007; revision submitted October 26, 2008.

preservation of strength in part of the liner during acceleration by a magnetic field, this criterion does not work. In this case, acceleration of the liner for a distance exceeding ten its thicknesses is possible. However, the perturbation growth will be determined by the complex dynamics of the loss of strength in part of the liner as a function of the development of instability since Joule heat release can increase in the inhomogeneity zone (in this case, the volume of the liner that have lost strength can differ from that obtained in one-dimensional calculations). As a result, it is difficult to predict how the instability during liner motion will develop.

Even for similar conditions of liner acceleration, the dynamics of development of Rayleigh–Taylor instability can differ significantly. Thus, in the liner experiments on the Shiva-Star facility at the U.S. Air Force Research Laboratory and on the Atlas facility at the Los-Alamos National Laboratories (USA) performed under similar conditions, radiographs of the liners indicate significant differences in the development of instability [4, 8]. In the series of Near Term Liner Experiments (NTLX) on the Shiva-Star and in the Hydro-Features (HF) experiments on the Atlas, the radiographs show a moderate or weak development of instability, whereas in the experiments of the Liner Demonstration (LD) series on the Atlas, significant development of instability was recorded.

Investigation of liner instability in the experiments by two-dimensional calculations and estimations [4, 8, 9] has shown that a theoretical explanation of the different behavior of liners in these experiments is a difficult problem and even a small difference in the formulation of the problem can have a significant influence on calculation results. Nevertheless, direct two-dimensional numerical magnetohydrodynamic (MHD) calculations of perturbation growth [9] have shown that the conditions of the HF and NTLX experiments lead to a smaller perturbation growths than the conditions of the LD experiments if this growth is determined from the degree of perturbation growth on the inner surface. A comparison of the calculated shape of the liner outer surface for the HF and LD experiments shows that, in the calculations, just as in the experiments, the HF liner remains slightly deformed and LD liner is severely deformed. Figure 1 gives the calculation results for the liners obtained in [9]. In the LD and NTLX experiments, the shapes of the outer surface of the liners remain qualitatively similar and highly perturbed even when using a maximally fine grid. Thus, the question of the stability of motion of condensed liners requires further investigation.

The purpose of the present work was to analyze the possible designs of experiments on the Atlas facility to study the physics of imploding liners. For studies of the development of instabilities, three experimental designs are proposed that can provide more stable motion of liners from a theoretical–computational point of view. If the results of experiments confirm the theoretical predictions of the greater stability of liner implosion under these conditions, this will mean first, that the assumptions and theoretical–computational models are valid, and, second, that the proposed methods are effective for preventing instabilities.

In the first design of the problem, in comparison with the LD experiments, in which unstable motion of liners was observed, it is proposed to decrease the initial liner radius R (from 5 to 3 cm) without changing its mass. Calculations have shown that this could provide the same liner velocities as in the LD experiments for the same radius of the measuring unit equal to 1 cm. However, since the aspect ratio R/δ (δ is the liner thickness) will considerably decrease in this case (the number of the thickness traveled by the liner will decrease), one might expect more stable liner motion. To confirm these assumptions, it was required to perform direct two-dimensional numerical calculations of liner acceleration with the perturbation growth taken into account.

In the second design, it is proposed to produce periodic perturbations at a certain wavelength on the outer surface of the liner, so that, during acceleration, the perturbations have no time to destroy the liner but can effectively suppress the growth of chaotic perturbations. There are a number of experimental data indicating that large-scale increasing perturbations can suppress the growth of chaotic perturbations of smaller scale. For example, in experiments studying Rayleigh–Taylor instability, the observed bubble surface [10, 11], as a rule, remains smooth enough, without visible perturbations, although it should be unstable according to the criteria of development of this instability. A second example is an increase in the amplitude of periodic perturbations in liners [12] to very large values (much exceeding the wavelength and comparable to the liner thickness) without significant distortions due to chaotic perturbations. Further evidence for the suppression of growth of small-scale perturbations by large-scale perturbations is the fact that, in contrast to quiescent fluid, the presence of growing perturbations results in a velocity shift and, hence, in stretching of small-scale perturbations and suppression of their growth.

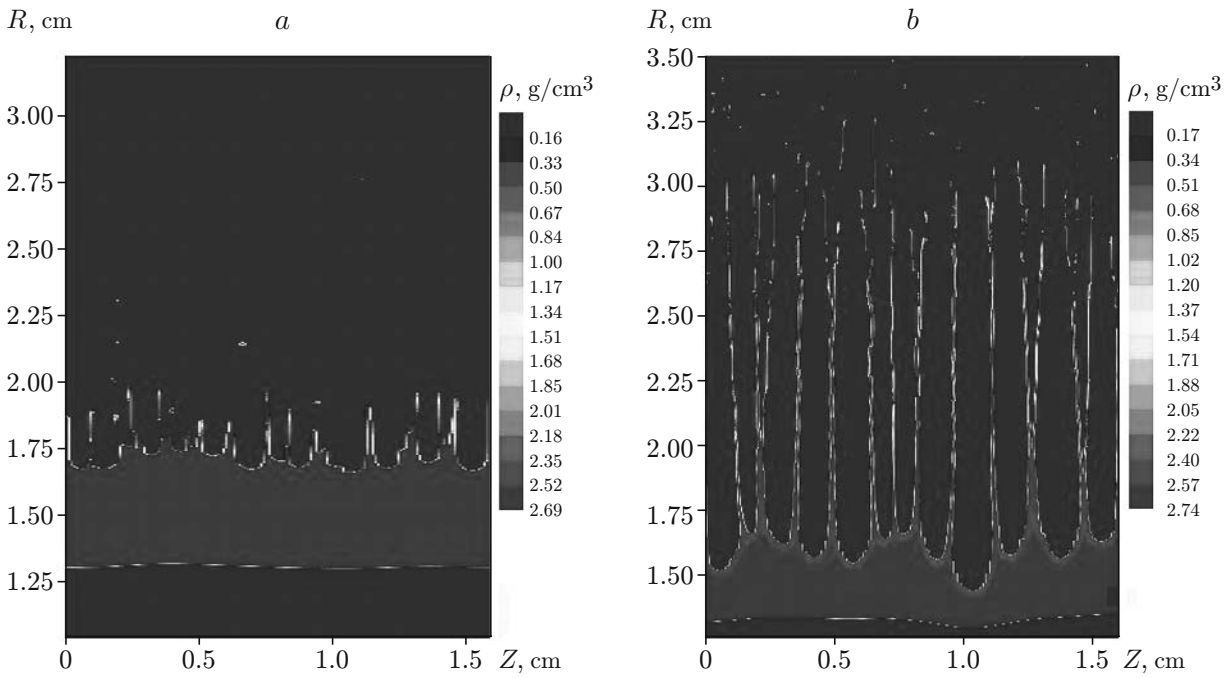

Fig. 1. Liner density isolines obtained in the calculations of HF (a) and LD (b) for the time corresponding to the position of the liner inner surface $R_{\text{in}} = 1.3$ cm.

The third version of the design is based on the use of the magnetic stabilization effect. The stabilization of Rayleigh–Taylor instability during magnetic acceleration of a liner due to Maxwell tension of magnetic lines was predicted theoretically in [13] taking into account the results of [14]. Experimentally, the existence of this effect was confirmed in the liner experiment on the Pegasus-2 facility [15]. The stabilization considered has pronounced anisotropy. If the direction of the grooves cut on the liner surface coincides with the magnetic field direction, the stabilization effect is absent. If the direction of the grooves is perpendicular to the magnetic field direction, the presence of the indicated effect is responsible for the maximum decrease in perturbations growth rate (to zero for short-wave perturbations at wavelength $\lambda < 4\pi\delta$). Generally, for an angle θ between the direction of the grooves and the magnetic field direction, the stability condition is given by the formula $\lambda < 4\pi\delta \sin^2\theta$ [14].

In the case of ordinary turning of the liner with surface, the grooves have the form of a cylindrical helix with a step nearly equal to zero, which corresponds to an almost zero value of the angle θ, i.e., to the absence of magnetic stabilization. We note that, in experiments [15], the angle of inclination of the grooves was equal to $\theta = 45°$. The question arises: can the finishing of the outer surface of the liner be changed so that, instead of having the azimuthal direction ($\theta = 0°$), the grooves are directed at an angle θ of about of 45° (grooves in the form of a cylindrical helix with a step comparable to the liner diameter) or at an angle $\theta = 90°$ (grooves along the z axis)? If, technologically, this is possible, it is of interest to perform an experiment with such a liner.

1. EFFECT OF ASPECT RATIO ON THE DEVELOPMENT OF LINER INSTABILITY

1.1. Results of One-Dimensional Calculations. We study the possibility of decreasing the initial radius of the liner with the preservation of its mass, height (4 cm), and velocities on the reception radius (equal to 1 cm) in the LD series of experiments. In these experiments, cylindrical liners (initial radius 5 cm; liner thickness 0.13 cm) were accelerated by an azimuthal magnetic field produced by time-dependent generator currents in the Z-pinch geometry. In different experiments of this series, the shapes of current curves differed only slightly (typical curve 1 in Fig. 2).

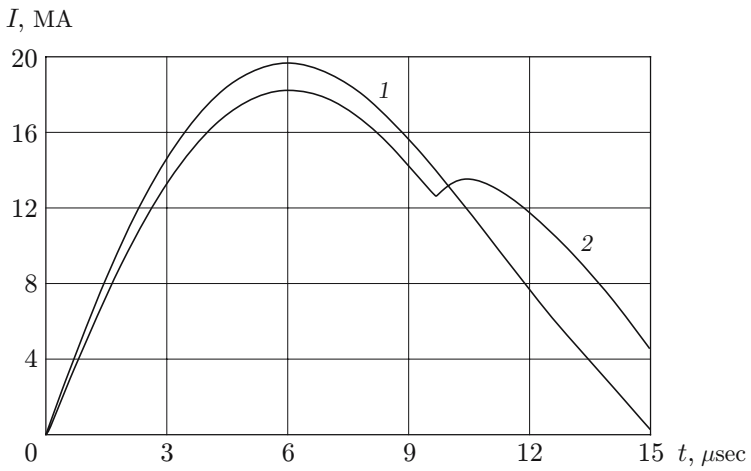

Fig. 2. Shape of current curves for the LD (1) and LDR experiment (2).

It is proposed to decrease (in comparison with the LD experiments) the initial liner radius to 3 cm. Then, with the unchanged mass of the liner, its thickness will be $\delta = 0.23$ cm. One-dimensional numerical simulation of the implosion of a liner with such initial radius and thickness (below, this experiment will be called LDR) was made using a software [7] with the equation of state and conductivity of aluminum taken from [16].

The system of MHD equations in the variables (r, z) for a magnetic field with one azimuthal component is in Lagrangian coordinates in the form

$$\frac{d\rho}{dt} + \rho \operatorname{div} \boldsymbol{v} = 0,$$

$$\rho \frac{d\boldsymbol{v}}{dt} = -\nabla p - \frac{1}{8\pi r^2} \nabla (Br)^2 + \operatorname{div} S,$$

$$\rho\Big(\frac{de}{dt} + p \frac{d\,(1/\rho)}{dt}\Big) = \Big(\frac{c}{4\pi}\Big)^2 \frac{(\nabla(Br))^2}{\sigma} + S_p(SD),$$

$$\rho \frac{d\,(B/\rho r)}{dt} = \operatorname{div}\Big(\frac{c^2}{4\pi\sigma r^2} \nabla(Br)\Big),$$

where c is the velocity of light, ρ, e, and p are the density, internal energy, and pressure, respectively, $\boldsymbol{v}$ is the velocity, B is the magnetic field, σ is the conductivity, S is the stress tensor deviator, D is the strain rate tensor, and $S_p(SD)$ is the first invariant of the SD tensor.

In the calculations, the following boundary conditions were imposed: the condition of rigid smooth walls $v_z = 0$, $\partial B/\partial z = 0$ on the side surfaces of the liner, the condition of free boundary and a current value $p = 0$ and $B = 2I/(cr)$ on the outer boundary of the liner, and the conditions of zero values of the radial velocity component and magnetic field $v_r = 0$ and $B = 0$ on the axis.

It was assumed that, at the initial time, the magnetic field in the liner was equal to zero and the liner was in rest ($\boldsymbol{v} = 0$). The temperature of the liner was set equal to room temperature $T = 293$ K, and the normal density $\rho = 2.7$ g/cm^3.

In an one-dimensional case where $v_z = 0$ and all quantities depend only on r, in the above system of equations, $\nabla = \partial/\partial r$ and $\operatorname{div} = (1/r)(\partial/\partial r)r$. Strength effects were ignored.

The one-dimensional calculations were performed using a code [7] with splitting into processes. The hydrodynamic equations were calculated by implicit schemes and magnetic diffusion was calculated by implicit schemes with flow marching.

The two-dimensional calculations were performed with the MIMOZA code [17, 18]. The two-dimensional equations were solved in two steps (Lagrangian and Eulerian). In the Lagrangian step, it was assumed that the difference grid nodes were frozen into the material and moved together with it. In the Eulerian step, conversion

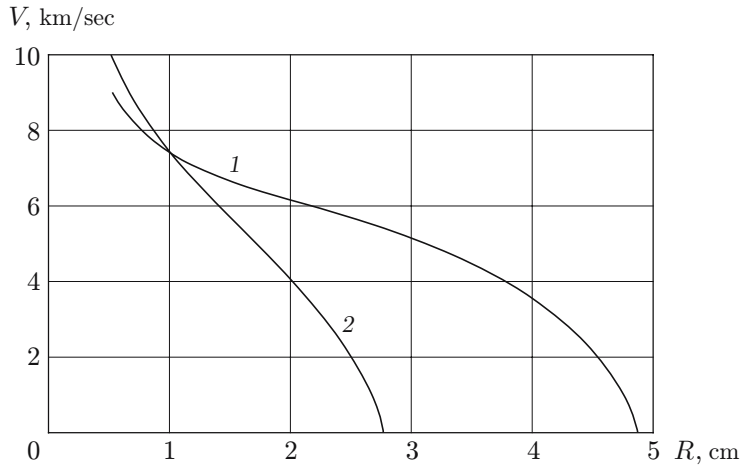

Fig. 3. Velocity of the liner inner surface versus radius for LD (1) and LDR (2) calculations.

of the quantities form the Lagrangian to Eulerian grids was performed. The algorithm is based on splitting into directions with the use of a one-dimensional algorithm of the second order of accuracy.

The equation of state used in the calculations is of analytical form. In this equation, the pressure is p and the specific internal energy e is the sum of three terms dependent on the temperature T and density ρ: a cold or an elastic component (dependent on the condensed density, sound velocity, and the energy of sublimation); a hot component (determining the equation of state for high temperatures or low densities) which coincides with the Saha equation of state for a multiply ionized plasma [19]; and a grid component of the form $e_3 \sim p_3/\rho \sim T^\alpha/\rho^\beta$, where $\alpha < 1$; $\beta < 0$ [this term makes a contribution to the thermal conductivity of the condensed material and decreases (compared to the second term) at high temperatures or low densities in the plasma region]. The first and third terms of the equation of state satisfy the thermodynamic identity exactly; therefore, the error of the identity is determined only by the Saha equation and should be small. In the case of using this equation in the code, two-phase states and, hence, the Maxwell rule are usually ignored, and it is assumed that, in unstable states ($\partial p/\partial\rho < 0$) in different computation meshes, the material will itself break up into a gaseous and a condensed phases. An advantage of this approach is that, in the calculations, the material in the two-phase region is inhomogeneous, in agreement with reality.

In the calculations, the material resistance in the plasma and condensed states is given by different formulas. The material resistance in the plasma state is considered to be Spitzer resistance with corrections for nonideality and with the electron scattering by neutral atoms taken into account. The material resistance in the condensed state is considered proportional to the internal energy and inversely proportional to density. For intermediate states, interpolation over the values of the material resistance for the condensed and plasma states is used.

In the LDR calculation, the current in the Atlas facility was varied according to its electrotechnical circuit. The circuit parameters are close to the parameters in the LD experiments (the capacitor bank charge voltage is approximately 160 kV, the initial load inductance is 26 nH). The shape of the obtained current curve (curve 2 in Fig. 2) differs slightly in shape from the curve in the LD experiments, primarily due to the higher inductance introduced during liner implosion.

Figure 3 gives curves of the velocity of the liner inner surface versus radius obtained in the LD and LDR calculations. The calculated current curves correspond to those presented in Fig. 2. In Fig. 3, it is evident that, as the initial liner radius is decreased without a change in its mass, the velocity of its inner boundary on a reception radius equal to 1 cm does not change. This is due to the fact that in the LD calculations, liner acceleration occurs primarily in a segment where the current value decreases (for a liner radius equal to 2 cm, the current it is approximately equal to 8 MA), and in the calculations LDR on a long segment of liner acceleration, the current is nearly maximal (for a liner radius equal to 2 cm, the current is approximately 18 MA).

Since the dynamics of development of Rayleigh–Taylor instability should be significantly affected by the Joule heat distribution in the skin-layer of the liner and the thickness of the melting zone, it is of interest to study

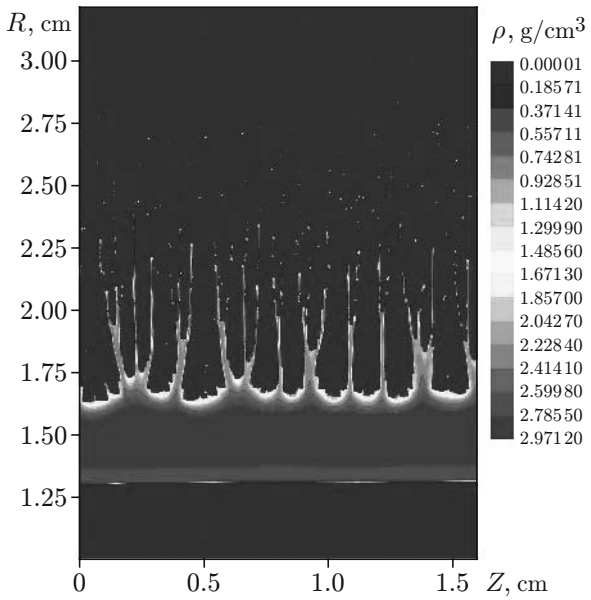

Fig. 4. Liner density isolines obtained in the LDR calculation for time $t = 7.83$ μsec, corresponding to the position of the liner inner surface $R_{\text{in}} = 1.3$ cm.

the spatial distribution of MHD quantities over the liner. Although in the LDR calculations with decreasing liner radius, the Joule heating of the outer surface is significantly higher (for example, in the LD calculations for a liner radius of 2 cm, the surface temperature is 0.26 eV, and for a smaller initial radius, it is 0.46 eV), the zone in which the temperature exceeds 0.1 eV, which approximately corresponds to melting, decreases, and for a liner radius of 2 cm, its mass is 37% of the liner mass, whereas in the LD calculations, it is 44%. Thus, with decreasing initial liner radius, its state is less subject to instability.

1.2. Two-Dimensional MHD Simulation of Perturbation Growth. To study the stability of liner motion, we performed two-dimensional numerical calculations of liner acceleration with the perturbation growth taken into account. The calculations were performed for two-dimensional (r, z) geometry on an Eulerian grid taking into account the material strength using the elastoplastic model, softening during melting, resistive diffusion, and Joule heat release.

The liner motion was calculated using the current curve for the LDR experiments (curve 2 in Fig. 2).

In the calculations, initial perturbations with a magnitude determined by the resolution of the grid used in the numerical calculations Δ were considered random. The theoretical arguments given in [9] show that the error arising in this case is insignificant. Actually, the error will be insignificant if the grid resolution (and, hence, the perturbation size) is sufficiently low. Therefore, it is necessary to perform calculations for convergence with decreasing Δ. This will provide evidence that the calculation results vary insignificantly with decreasing size of the grid mesh.

As shown by the calculations, the wavelength λ_m of the most rapidly developing perturbations in the LD experiment is approximately equal to 4 mm. To include the most dangerous perturbation modes in the calculation, the width of the computation region was set equal to 1.6 cm, i.e., larger than the value of λ_m.

Figure 4 shows the density isolines obtained in the two-dimensional LDR calculations on a grid with a resolution $\Delta = 0.0025$ cm on the radius and 2Δ on the z coordinate. It is evident that, in the LDR calculations, the liner is less deformed than in the LD calculations (see Fig. 1b).

The calculations showed a significant difference in the degree of perturbation growth. The perturbation amplitude a, which is defined as half of the difference between the maximum and minimum (along the radius) positions of the inner surface $a \approx 0.0265$ cm in the LD calculation and $a \approx 0.0026$ cm in the LDR calculation, i.e., an order of magnitude smaller [with a decrease in the liner radius to 1 cm, the perturbation amplitude in the LDR calculation increases insignificantly ($a \approx 0.0031$ cm)].

Since the liner mass decreases due to the development of instability, the liner can be accelerated to higher velocities. For the LD experiment in the one-dimensional calculation, the velocity of the inner part of the liner on a radius of 1.3 cm is 6.9 km/sec, and in the two-dimensional calculation, the average (on the z coordinate) velocity of the inner part of the liner on this radius is 7.4 km/sec; for the LDR experiment, these values are 6.32 and 6.57 km/sec, respectively. Thus, in the calculation for the LDR experiment, the decrease in the liner mass is less significant.

2. DEVELOPMENT OF LINER INSTABILITY IN THE PRESENCE OF PERIODIC PERTURBATIONS

2.1. Choice of Periodic Perturbations. The wavelength λ^* and the initial amplitude a_0^* of the specified periodic perturbation were chosen subject to the following conditions: 1) during growth, the perturbation should not reach the inner boundary of the liner; 2) the perturbation amplitude should be large enough so that its effect on the growth of chaotic perturbations is significant; 3) the wavelength and amplitude of the periodic perturbation should be much larger than the wavelength and amplitude of the short-wave perturbations produced by the cutter during manufacture of the liner; 4) the initial amplitude a_0^* of the specified periodic perturbation should be on the order of the wavelength.

It should be noted that, if conditions 3 and 4 are satisfied, the growth Rate of short-wave perturbations can be decreased (compared to the wavelength of the periodic perturbation), at least, by reducing the normal component of the acceleration due to gravity on the sites of the surface between the humps and valleys of the periodic perturbation. In this case, the meaning of condition 4 is as follows: the larger the ratio of the amplitude to wavelength of the periodic perturbation, the more significant the decrease in the gravity. The effect of the velocity shift produced by the periodic perturbation on the growth of small-scale perturbations will also be the greater, the larger the amplitude of the periodic perturbations. The meaning of condition 3 (the condition that the periodic perturbations are large-scale compared to the chaotic perturbations) is as follows: the larger the wavelength λ^*, the larger fraction of the perturbations have wavelengths smaller than λ^*.

Because the interaction of perturbations of different wavelengths is nonlinear (in the examined stage, where the perturbations cannot be considered small), it is difficult to predict all or even the most significant consequences of this interaction. Therefore, a two-dimensional calculation with the addition of the periodic perturbation to the spectrum of random perturbations can be considered as a peculiar computing experiment. From experimental results [13], it follows that the growth of chaotic perturbations can also be suppressed by introducing periodic helical perturbations. However, numerical simulations of the effect of helical perturbations require three-dimensional calculations; therefore, such simulations are currently impossible.

To choose admissible parameters a_0^* and λ^*, we performed a series of approximate calculations of the growth of periodic perturbations. In these calculations, it was assumed that the amplitude begins to increase from the moment of melting (partial or complete) of the liner outer surface. For the nonlinear stage of perturbation growth ($a > 0.1\lambda^*$), the velocity of introduction of periodic bubbles into the liner was defined by the well-known formula $u \approx F_0\sqrt{\lambda^* g}$, where $F_0 = 0.24$, and g is the acceleration due to gravity (see, for example, [20]). In the calculation of the introduction of bubbles, we also took into account an increase in liner thickness during its convergence. The time dependence of the current was taken from the experiment whose results are given in Fig. 2. In the calculation of the liner acceleration, it was assumed that the effective mass of the liner decreases during the introduction of bubbles into it.

From the results of the approximate calculations in the above formulation, the following initial parameters of the periodic (sinusoidal) perturbation were chosen: $\lambda^* = 0.04$ cm and $a_0^* = 0.013$ cm

2.2. Two-Dimensional MHD Simulation of Perturbation Growth. The flight of the liner with periodic perturbations (LDP calculation) was simulated using the same current curve as for the LD experiment (curve 1 in Fig. 2). Thus, the results of one-dimensional calculations for the LDP experiment coincide with results for the LD experiment (see Fig. 3).

Figure 5a gives the results obtained in the two-dimensional LDP calculation on a grid with a resolution $\Delta = 0.0025$ cm on the radius and 2Δ on the z coordinate. The initial perturbations were the sum of sinusoidal perturbations with the parameters λ^* and a_0 indicated above and random perturbations distributed uniformly in

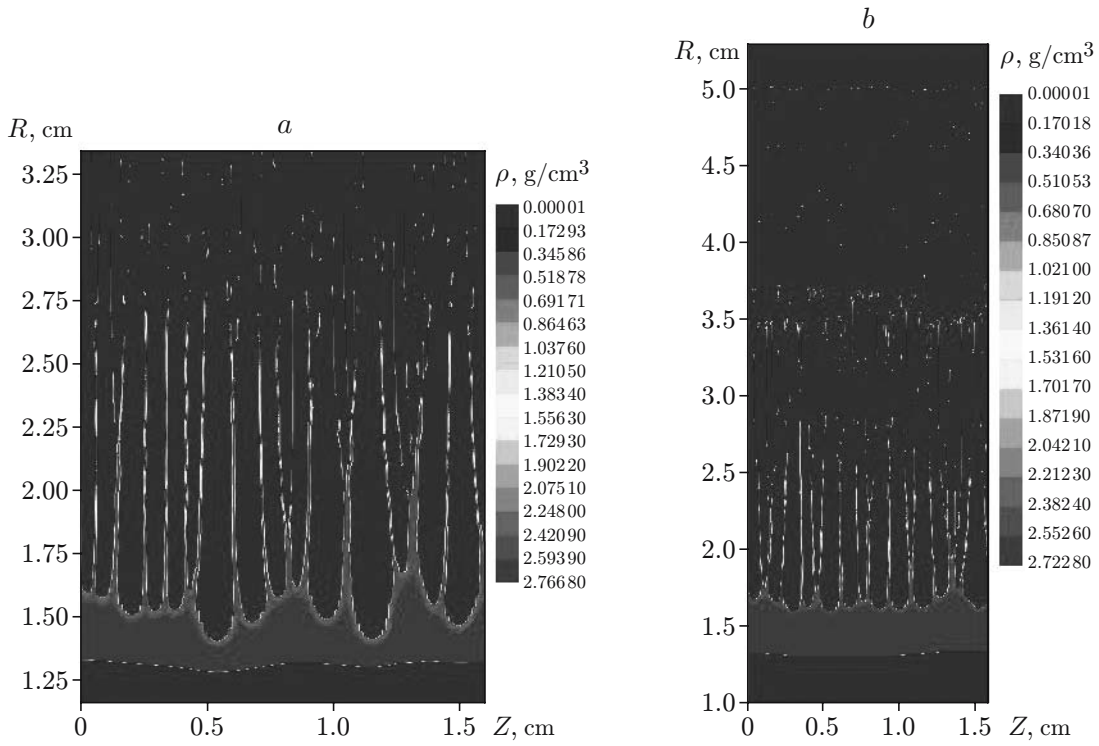

Fig. 5. Liner density isolines obtained in the LDP and LDP1 calculations for the times corresponding to the position of the liner inner surface $R_{\text{in}} = 1.3$ cm: (a) LDP ($t = 11.7$ μsec); (b) LDP1 ($t = 13.2$ μsec).

each mesh of the outer surface in the range from $-\Delta/4$ to $\Delta/4$.

From a comparison of Fig. 1b and Fig. 5a, it follows that, in the LDP calculation, the state of the liner is not less perturbed than that in the LD calculation. The degree of perturbation growth on the inner boundary in the LD and LDP calculations is approximately identical (in the LDP calculation, $a \approx 0.0273$ cm).

Due to a decrease in the liner mass resulting from the growth of periodic perturbations, the velocity of the liner inner surface is significantly higher (approximately 8.8 km/sec) in the LDP calculation than in the LD calculation. Thus, in the LD and LDP calculations, the properties of the liners are far from being identical. It can be assumed that the growth of chaotic perturbations with the preservation of the liner velocity can be stabilized by increasing the liner thickness during the generation of periodic perturbations.

In the LDP1 calculation, the liner thickness was increased to 1.6 mm and the same periodic perturbations as in the LDP calculation were produced on the liner surface, in addition to chaotic perturbations. The same current curve as in the LD calculation (see Fig. 2) was used. The results of the LDP1 calculations are presented in Fig. 5b.

In the LDP1 calculation, the liner velocity on a radius of 1.3 cm was 6.5 km/sec, which is slightly lower than the liner velocity in the one-dimensional LD calculations (6.9 km/sec), i.e., the liner thickness was excessively increased. In the LDP1 calculation, the degree of perturbation of the liner outer surface on the final radius was somewhat smaller than that in LDP calculation, and the perturbation of the inner boundary in the LDP1 calculation was approximately half ($a = 0.014$ cm) that in the LD and LDP calculations. Thus, by producing periodic perturbations on the liner surface and simultaneously increasing its thickness, it is possible to stabilize the growth of chaotic perturbations with the preservation of the properties of the liner.

CONCLUSIONS

Some design of experiments on the Atlas facility were considered to study the physics of liner implosion and determine the optimal conditions of stable motion of liners.

Direct two-dimensional numerical MHD calculations of perturbation growths showed that, decreasing the initial liner radius to 3 cm with the preservation of its mass (LDR calculation) led to a significantly smaller perturbation growth than that in the LD experiments if this growth was judged by the perturbation growth on the inner surface. This may be due to the fact that, in the LDR calculation, the liner travels a distance equal to a smaller number of its thickness and also due to the fact that a smaller part of liner is melted during acceleration. The comparison of the shapes of the outer surface obtained in the LDR and LD calculations showed that the outer surface of the LDR liner was also perturbed to a much smaller extent.

In the calculation for the LDP experiment, in which periodic perturbations are produced on the liner surface, the perturbation amplitude on both the inner and outer surface differs insignificantly from the amplitude obtained in calculations without periodic perturbations but the velocity on the reception radius increases due to of a more significant decrease in the liner mass during acceleration. If the liner thickness is increased during the production of periodic perturbations (LDP1 calculation), the growth of chaotic perturbations is somewhat stabilized (according to the calculation, the perturbations of the inner surface are twice smaller) with an insignificant change in the liner velocity. Such stabilization is not sufficiently reliable because of calculation errors but experimental verification of calculation results is nevertheless reasonable since this method of stabilization could become universal and independent on the degree of matching of the load to the current source.

It is also suggested that the liner flight in experiments on the Atlas facility can be stabilized by special processing of the liner surface.

This work was performed under a contract between the Los-Alamos National Laboratories (USA) and All-Russia Research Institute of Experimental Physics (No. 37713–000-02-35; Task Order 017).

REFERENCES

1. V. K. Chernyshev, V. N. Mokhov, M. S. Protasov, et al., "Liner ponderomotive units used as a driver in magnetic implosion systems," *Vopr. Atom. Nauki Tekh., Ser. Mat. Model. Fiz. Prots.*, No. 4, 42–50 (1992).
2. A. M. Buyko, V. V. Zmushko, P. N. Nizovtsev, et al., "On feasibility to achieve high longitudinal symmetry of cylindrical metal liners compressed by currents from most powerful disk EMG," in: C. Stallings and H. Kirbie (eds.), *Digest of Tech. Papers 12th IEEE Int. Pulsed Power Conf.*, Monterey (1999), pp. 1145–1148.
3. A. M. Buyko, O. M. Burenkov, V. V. Zmushko, et al., On the feasibility to achieve high pressures with disk EMG driven impacting liners," in: R. Reinovsky and M. Newton (eds.), *Digest of Tech. Papers: Pulsed Power Plasma Science-2001*, Inst. of Electric. and Electron. Eng., Inc. (2001), pp. 516–519.
4. R. E. Reinovsky, W. E. Anderson, W. L. Atchison, et al., "Pulsed power hydrodynamics: A new application of high magnetic field," in: V. D. Selemir and L. N. Plyashkevich (eds.), *Proc. of the 9th Int. Conf. on Megagauss Magnetic Field Generation and Related Topics* (Moscow–St. Petersburg, 2002), Inst. of Exp. Phys., Sarov (2004), pp. 696–705.
5. S. F. Garanin, V. I. Mamyshev, and V. B. Yakubov, "The MAGO system: current status," *IEEE Trans. Plasma Sci.*, **26**, No. 4, 2273–2278 (2006).
6. J. H. Degnan, T. Cavazos, D. Clark, et al., "On research on magnetic pressure implosions of long cylindrical liners, suitable for subsequent compression of the field reversed configuration type of compact toroids," in: V. D. Selemir and L. N. Plyashkevich (eds.), *Proc. of the 9th Int. Conf. on Megagauss Magnetic Field Generation and Related Topics* (Moscow–St. Petersburg, 2002), Inst. of Exp. Phys., Sarov (2004), pp. 730–737.
7. S. F. Garanin, G. G. Ivanova, D. V. Karmishin, and V. N. Sofronov, "Diffusion of a megagauss field into a metal," *J. Appl. Mech. Tech Phys.*, **46**, No. 2, 153–159 (2005).
8. W. L. Atchison, R. J. Faehl, I. R. Lindemuth, et al., "Dependence of solid liner stability on drive conditions during magnetic implosion," in: V. D. Selemir and L. N. Plyashkevich (eds.), *Proc. of the 9th Int. Conf. on Megagauss Magnetic Field Generation and Related Topics* (Moscow–St. Petersburg, 2002), Inst. of Exp. Phys., Sarov (2004), pp. 710–717.
9. A. M. Buyko, S. F. Garanin, D. V. Karmishin, et al., "Analysis of the liner stability in various experiments," *IEEE Trans. Plasma Sci.*, **36**, No. 1, 4–9 (2008).
10. O. I. Volchenko, I. G. Zhidov, E. E. Meshkov, and V. G. Rogachev, "Development of localized perturbations on the unstable boundary of an accelerated liquid layer," *Pis'ma Zh. Tekh. Fiz.*, **15**, No. 1, 47–51 (1989).
11. E. E. Meshkov, *Rayleigh–Taylor Instability: Laboratory Experiments*, Krasnyi Octyabr', Saransk (2002).

12. R. Reinovsky, W. Atchison, and W. Anderson, et al., "Stability of magnetically imploded liners for high energy density experiments," in: H. J. Schneider-Muntau (ed.), *Proc. of the 8th Int. Conf. on Megagauss Magnetic Field Generation and Related Topics* (Tallahassee, USA, 1998), World Sci., Singapore (2004), pp. 473–478.
13. S. F. Garanin, S. D. Kuznetsov, C. Ekdahl, et al., "On feasibility of Rayleigh–Taylor instability magnetic stabilization of liner implosions," in: J. Schneider-Muntau (ed.), *Proc. of the 8th Int. Conf. on Megagauss Magnetic Field Generation and Related Topics* (Tallahassee, USA, 1998), World Sci., Singapore (2004), pp. 563–566.
14. E. G. Harris, "Rayleigh–Taylor instabilities of a collapsing cylindrical shell in a magnetic field," *Phys. Fluids*, **5**, No. 9, 1057–1062 (1962).
15. B. G. Anderson, W. E. Anderson, A. M. Buyko, et al., "Liner experiment on verification of Rayleigh–Taylor instability magnetic stabilization effect (joint LANL/VNIIEF experiment PEGASUS-2)," in: R. Reinovsky and M. Newton (eds.), *Digest of Tech. Papers: Pulsed Power Plasma Science-2001*, Inst. of Electric. and Electron. Eng., Inc. (2001), pp. 354–355.
16. A. M. Bujko, S. F. Garanin, V. A. Demidov, et al., "Investigation of the dynamics of a cylindrical exploding liner accelerated by a magnetic field in the megagauss range," in: V. M. Titov and G. A. Shvetsov. *Megagauss Fields and Pulsed Power Systems*, Nova Sci. Publ., New York (1990), pp. 743–748.
17. I. D. Sofronov, S. A. Bel'kov, O. A. Vinokurov, et al., "Complex of MIMOZA-99 codes," in: *Trans. of the All-Russia Research Institute of Experimental Physics*, All-Russia Research Institute of Experimental Physics, Sarov, (2001), pp. 94–101.
18. A. M. Buyko, S. F. Garanin, V. V. Zmushko, et al., "2D computations for perturbation growth of magnetically driven cylindrical aluminum and aluminum alloy liners," in: E. Meshkov, Yu. Yanilkin, and V. Zhmailo (eds.), *Proc. of the 7th Int. Workshop Phys. Compressible Turbulent Mixing* (St. Petersburg, Russia, 1999), Inst. of Exp. Phys., Sarov (2001), pp. 237–243.
19. Ya. B. Zel'dovich and Yu. P. Raizer, *Physics of Shock Waves and High-Temperature Hydrodynamic Phenomena*, Academic Press, New York (1967).
20. P. R. Garabedian, "On steady-state bubbles generated by Taylor instability," *Proc. Roy. Soc. London, Ser. A*, **241**, p. 423 (1957).